A EUROPEAN JOURNAL

CHEMPHYSCHEM

OF CHEMICAL PHYSICS AND PHYSICAL CHEMISTRY

Accepted Article

Title: Optoelectronic Temporal Stability of Metal Chloride-Doped CVD Graphene

Authors: Moon H Kang; William Ireland Milne; Matthew Thomas Cole

To be cited as: ChemPhysChem 10.1002/cphc.201600260

Link to VoR: http://dx.doi.org/10.1002/cphc.201600260

A Journal of

ChemPubSoc Europe

www.chemphyschem.org

WILEY-VCH

ARTICLE WILEY-VCH

Temporal Stability of Metal Chloride-Doped CVD Graphene

Moon H. Kang,*[a] William I. Milne,[a, b] & Matthew T. Cole*[a]

Abstract: Graphene has proven to be a promising material for transparent flexible electronics [1]. In this study, we report on the development of a transfer and doping scheme of large-area chemical vapour deposited (CVD) graphene. A technique to transfer the as-grown material onto mechanically flexible and optically transparent polymeric substrates using ultra-violet adhesive (UVA) is outlined, along with the temporal stability of the sheet resistance and optical transparency following chemical doping with various metal chlorides (M_xCl_y); gold chloride ($AuCl_3$), ferric chloride ($FeCl_3$), tin chloride ($SnCl_2$), iridium chloride ($IrCl_3$) and rhodium chloride ($RhCl_3$). The sheet resistance (R_S) and 550 nm optical transparency ($\%T_{550}$) of the transferred undoped graphene was 3.5 kΩ/sq. (±0.2 kΩ/sq.) and 84.1% (±2.9%), respectively. Doping with $AuCl_3$ showed a notable reduction in R_S by some 71.4 % (to 0.93 kΩ/sq.) with a corresponding $\%T_{550}$ of 77.0%. After 200 hours', exposure to STP air, the increase in R_S was found to be negligible ($\triangle R_S^{AuCl3}$ = 0.06 kΩ/sq.) indicating that, of the consider M_xCl_y, $AuCl_3$ doping offered the highest degree of time stability under ambient conditions. There appears a tendency for increasing R_S with time for the remaining metal chlorides studied. We attribute the observed temporal shift to desorption of molecular dopants. We find that the desorption was most significantly in $RhCl_3$-doped samples ($\Delta\Gamma/\Gamma_0$ = -1.064), whilst, in contrast, after 200 hours in ambient, $AuCl_3$-doped graphene showed only marginal desorption ($\Delta\Gamma/\Gamma_0$ = 0.019). The results of this study demonstrate that chemical doping of UVA and HPL transferred graphene is a promising means for enhancing large-area CVD graphene to offer a viable platform for next generation flexible electronics.

Introduction

Indium- and Fluorine- tin oxide (ITO / FTO) have gained significant market traction as transparent electrodes in large-area electronics. Though concurrently offering high optical transparency and high electrical conductivity, such oxides are, however; particularly brittle [2]. Graphene, an atomically thin layer of hexagonally latticed carbon atoms, has been widely proposed an as alternative. Graphenes' high charge mobility, high optical transmittance, alongside its impressive mechanical robustness and flexibility make it well-suited for a number of emerging opto-electronics applications, such as e-paper, flexible displays and user-conformal wearables [3]. To date there have been many attempts to utilize graphene as a transparent flexible conductor in organic light emitting diodes (OLED), [3b, 4] touch screens [5] and photovoltaic cells [6]. Common to all such opto-electronic applications is the need for a reduction in the graphene's sheet resistance (R_S) whilst maintaining its high optical transparency. Unlike normal metals, graphene has a conical band structure [3]. The Fermi level of pristine graphene lies at the Dirac point, where there is a significantly reduced, and theoretically null, density of states. Due to this low density of states, the R_S of monolayer pristine graphene is fundamentally limited to a few kΩ/sq. This is industrially deemed too high for use in most commercial applications; touch screens require R_S <500 Ω/sq., whilst graphical displays require R_S <100 Ω/sq, for flat band transparencies > 90% across the optical spectrum[7]. One approach to reducing R_S is to shift the Fermi level by selective doping.

Chemical doping has been considered one of the most viable means of decreasing R_S without compromising graphene's as-synthesised optical transparency.[8] In the present study we adopted a chemical doping methodology based on established chlorine compounds that have been investigated elsewhere in other nanocarbon systems [8c, 8f, 9]. The spatial and temporal variation in the sheet resistance and optical transparency are investigated. Doping samples showed only a small decay in performance ($AuCl_3$: 9% decrease in R_S), even after exposure to air for 200 h, highlighting the potential of two-dimensional-material based opto-electronic devices.

Results & Discussion

Graphene was grown by CVD and transferred onto PET substrates using an inherently scalable UVA-transfer method, as reported in further detail elsewhere[10]. Following UVA-transfer the graphene was chemically doped with one of five chloride

[a] *M. H. Kang, *Dr. M. T. Cole, Prof. W. I. Milne
Electrical Engineering Division, Department of Engineering
University of Cambridge
CB3 0FA, Cambridge, United Kingdom
E-mail: mhk29@cam.ac.uk, mtc35@cam.ac.uk

[b] Prof. W. I. Milne
College of Information Science and Electronic Engineering,
Zhejiang University,
310027, Hangzhou, P. R. China
E-mail: wim1@cam.ac.uk

compounds ($AuCl_3$, $FeCl_3$, $SnCl_2$, $IrCl_3$, or $RhCl_3$) to enhance its conductivity. For this chemical doping, each compound was dissolved in different solvents ($AuCl_3$ and $IrCl_3$ / acetonitrile, $FeCl_3$ and $SnCl_2$ / DI water, and $RhCl_3$ / methanol) each at 20 mM concentration. The dopant solutions were spin-cast onto the transferred graphene samples at 2000 rpm for 1 min.

To assess the implications of the M_xCl_y doping it is necessary to decouple any shifts in R_s and %T due to the solvent from those of the M_xCl_y solute. Figure 1 sumarises the solvent and concentration controls. In the solvent controls three high-purity solvents (DI water, methanol, and acetonitrile) were spin-coated on the graphene using the casting same recipe as those used for the M_xCl_y doping and optical transmittance (%T) and sheet resistance (R_S) measured.

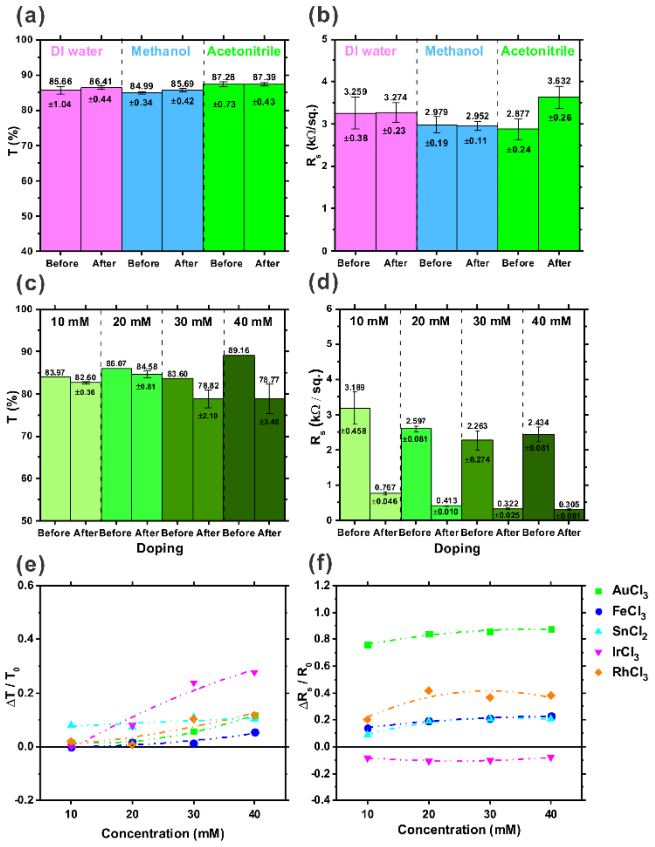

Figure 1. Solvent controls: (a) optical transmittance (550 nm) and (b) sheet resistance of graphene on PET following solvent treatment (without dopant). (c) optical transmittance (550 nm) and (d) sheet resistance of $AuCl_3$-doped graphene for various molar concentrations. (e) Normalised optical transmittance change and (f) sheet resistance change of graphene doped for all M_xCl_y as a function of molar concentrations.

As shown in Figure 1(a) and (b), there was no significant change in %T (Δ%T = +0.75 %, +0.7 %, and +0.11 %) for samples treated with DI water, methanol and acetonitrile, respectively. Similarly, there was no significant change in R_S (ΔR_S = +0.013 kΩ/sq., -0.027 kΩ/sq.) for samples treated with DI water, and methanol, respectively, however samples treated with acetonitrile showed a non-negligible increase in R_s (+0.245 kΩ/sq.). Acetonitrile degrades R_s. In the present study $AuCl_3$ was dissolved in acetonitrile in our M_xCl_y doping studies. Interesting, our $AuCl_3$ samples showed the largest decrease in R_s, even though the doping effects of acetonitrile evidently tend to increase R_s. One beneficial strategy to further improve the doping effects of $AuCl_3$ is to use alternative solvents. Nevertheless, Figures 1(a) and (b) broadly reveal that the impact of the solvent is largely negligible and suggest that the observed variations in R_S and %T, upon M_xCl_y doping, are not attributed to the solvent but rather the solute. Figure 1(c) and (d) show the %T and R_S of the doped graphene as a function of various concentrations of $AuCl_3$. As the dopant concentration increased, the doped graphene showed lower %T and lower R_S. %T was substantially decreased (Δ%T = 10.39%) at 40 mM, even though the R_S was not notably decreased with R_s, which had a comparable value to the reduction at 30mM (ΔR_S = 1.941 kΩ/sq) and 20 mM (ΔR_S = 2.184 kΩ/sq). The normalised Δ%T and ΔR_S of doped graphene on PET with the five kinds of dopant solution, as shown in Figure 1(e) and (f), suggest that R_S is not direct proportional to dopant concentration, whilst the %T decreases consistently with increasing the concentration. This results indicate that the dopant molecules may adsorb on the graphene surface resulting in a %T decrease, but the charge transfer from the dopant molecules evidently saturate at concentrations in excess of 20 mM. The reduction in R_S appears to relate to the degree of electronegativity of the metal ions[11]. As shown in Figure 1(f), the largest reduction in R_S ($\Delta R_S/R_0$ = 0.841) was observed from the $AuCl_3$-doped which has the highest electronegativity (2.54) of the dopants considered ($FeCl_3$: 1.83, $SnCl_2$: 1.96, $IrCl_3$: 2.2, and $RhCl_3$: 2.28). Similar trends in R_s and

metal constituent electronegativity where noted throughout. Additional transport studies will be reported elsewhere.

Chemical doping was adopted because it does not induce significant mechanical modification of the graphene backbone, unlike substitutional doping which is often achieved through aggressive plasma-based processing. The in-solution metal chloride molecules mediate effective charge transfer to the graphene basal plane. The molecules are physically adsorbed mediating spontaneous charge transfer across well-defined energy levels at the graphene-metal ion interface. In the present system the expected reaction between the metal chloride and graphene is; [9a]

$$\text{Graphene} + 3\text{MeCl}_3 \rightarrow \text{Graphene} + \text{MeCl}_2^- + \text{Me(I)} + \text{MeCl}_4^- \quad (1)$$

$$\text{MeCl}_2^- \rightarrow \text{Me}^0 + 2\text{MeCl}_4^- \quad (2)$$

$$\text{MeCl}_4^- + \text{Graphene} \rightarrow \text{Grahpene}^+ + \text{Me}^0 \quad (3)$$

The positive Me^{3+} ions in $MeCl_4^-$ have a tendency to be neutralized following charge donation to the graphene. Depending on the metal type, the positive reduction potentials of the metal ions result in the removal of a given proportion of the local electrons populations from the graphene substrate, thereby mediating *p*-type doping. The dispersed $SnCl_2$ interaction differs from the other four considered metal chlorides. Since $SnCl_2$ reacts in H_2O, producing Sn(OH)Cl and HCl [12], we note that;

$$\text{Sn(OH)Cl} + \text{HCl} + \text{Graphene} + \text{O} \rightarrow \text{SnO}_2 + 2\text{HCl} + \text{Graphene}^- \quad (4)$$

The aqueous $SnCl_2$ behaves as a reducing agent. Sn^{2+} reacts with bound oxygen species, deposited during ambient exposure, on the graphene. When the oxygen constituent is removed the graphene becomes increasingly negatively charged, leading to *n*-type doping. The Sn^{2+} oxidation standard potential is negative (-0.19 V)[13]; it has a tendency to donate electrons to the graphene substrate, whereas the remaining four dopants have positive potentials ($AuCl_3$: 1.002 V, $FeCl_3$: 0.77 V, $IrCl_3$: 1.156 V, and $RhCl_3$: 0.76 V)[13]. Thus, graphene doped with $AuCl_3$, $FeCl_3$, $IrCl_3$ and $RhCl_3$ will likely show nominally *p*-type behaviour, whereas $SnCl_2$ doped graphene would exhibit nominally *n*-type behaviour. Indeed, our Raman spectroscopy findings (2D-peak shift: 14.64 cm^{-1}($AuCl_3$), 2.86 cm^{-1}($FeCl_3$), -2.04 cm^{-1}($SnCl_2$), -4.54 cm^{-1}($IrCl_3$), and 1.30 cm^{-1}($RhCl_3$)) do indeed largely confirm this thesis. The anomalous Raman behaviour of $IrCl_3$ is under further investigation. Although the charge polarity of the doped graphene varies, it remains true that all the various metal chlorides studied induce an increase in the charge carrier population, thereby increasing the carrier density and hence a lowering of the sheet resistance. Additionally, consistent with reports elsewhere, we find that the dopant molecules are prone to adhere to defects, vacancies, grain boundaries and other high surface potential non-idealities within the graphene basal plane. Chang *et. al.* showed that adatoms on graphene have a tendency to dwell on atomic steps or boundaries[14]. Though degrading the lattice periodicity, the readily adsorbed dopant molecules easily bind to boundaries and cracks and manifestly heal them, increasingly additional charge transport routes, especially throughout particularly defective micro areas.

Figure 2(a) and (b) are photographs of 20 mm x 20 mm as-grown graphene on Cu foil and UVA-transferred samples. Figures 2(c) and (d) show the spatial variation in the optical transmittance (%T at 550 nm) (ATI, Unicam UV2) and Figure 2(e) and (f) display the sheet resistance variation of undoped and $AuCl_3$-doped graphene, Full spectra were acquired at each measured position. Figure 2(g) summarises the mean %T maps for all the dopants considered. The $\%T_{550}$ of the undoped graphene was 84.1%, some 5.2% lower than that in bare PET (89.3%), suggesting that the graphene is largely monolayer, as corroborated by our polychromatic Raman analysis where we got a I_D/I_G ~ 2.05 and I_{2D}/I_G ~ 0.29 with the remaining optical absorption associated with the 5 µm-thick UV-adhesive. The standard deviation in the spatially resolved %T of the undoped graphene on PET suggests that transfer method led to an areal uniformity of ca. 2.9% resulting in an optical absorption ranging from 2.3% to 8.1% across the sample (20 mm X 20 mm). After chemical doping, the areal mean $\%T_{550}$ decreased by 7.0% ($RhCl_3$-doped), 19.2% ($IrCl_3$-doped) 7.1 % ($AuCl_3$), 7.5%, ($FeCl_3$) and 10.3% ($SnCl_2$).

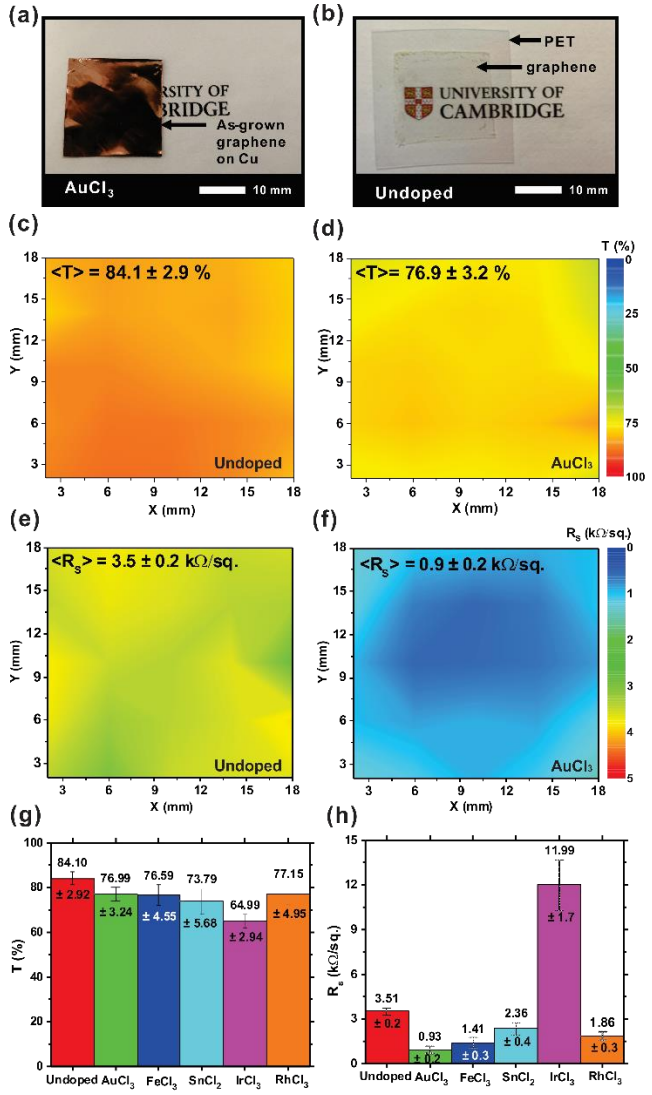

Figure 2. Photographs of typical (a) as-grown graphene on Cu foil and (b) transferred graphene onto PET, optical transmittance maps (550 nm) of (c) undoped graphene, and (d) $AuCl_3$-doped graphene, Sheet resistance maps of (e) undoped graphene and (f) $AuCl_3$-doped graphene, and Bar charts of mean values of (g) optical transmittance and (h) sheet resistance of undoped and 5 metal chloride-doped graphene.

Figure 2(e) and (f) show the spatially resolved sheet resistance (Jandel Four-Point Probe) of the undoped and doped graphene on PET. The UVA-transferred graphene showed a sheet resistance of 3.5±0.2 kΩ/sq. By way of a control, to compare the R_S of the UVA-transferred graphene to that of conventional PMMA-transfer we assessed the conductivity of as-grown graphene independently by transferring it to quartz substrates. The transferred graphene showed a sheet resistance of 5.5±1.2 kΩ/sq., which is some 64% higher than that of UVA transferred graphene. Clearly the transfer method plays a critical role in optimising R_S. As shown in Figure 2(h), $AuCl_3$-doping afforded the lowest R_S (0.9±0.2 kΩ/sq.), showing a rather dramatic decrease ($\triangle R_S$ = 2.6 kΩ/sq.). The highest R_S was for the $IrCl_3$-doped graphene (12.0±1.7 kΩ/sq.). Graphene electrodes are attractive for the flexible display industry; however spatial uniformity in R_S is key if such materials are to be adopted widely in display panels. The R_S and its spatial uniformity intimately dictate light emission uniformity. Following UVA transfer, the R_S spatial distribution (measured over4 cm^2) for the undoped graphene was found to be very uniform (±0.2 kΩ/sq.), which was maintained even after chemical doping with $AuCl_3$ (±0.2 kΩ/sq.), $FeCl_3$ (±0.3 kΩ/sq.), $SnCl_2$ (±0.4 kΩ/sq.), and $RhCl_3$ (±0.3 kΩ/sq.). The transfer, rather than the growth or doping procedure, dominates the spatial uniformity in R_S. However, the distribution of the R_S standard deviation in the $IrCl_3$-doped (±1.7 kΩ/sq.) was significantly higher than in the undoped case (±0.2 kΩ/sq.) suggesting that, in such systems, the doping procedure dominates the final uniformity. SEM inspection suggests that the agglomeration of large Ir precipitates, some 14.4±3.7 μm in diameter, is the likely cause for this reduced spatial uniformity, with the other Me_xCl_y precipitates being some 10 times small on average. $AuCl_3$ is the most effective dopant showing a markedly lower R_S (0.9±0.2 kΩ/sq.) with only a 7.1% decrease in optical transmittance (Figures 2(g) and (h)).

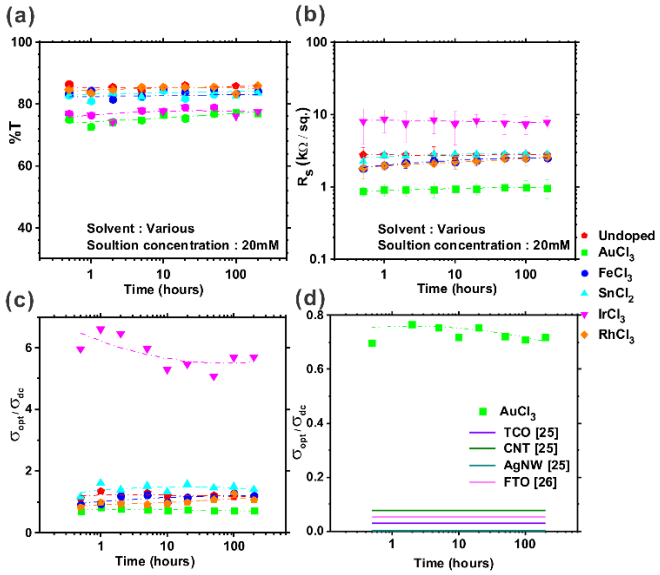

Figure 3. Time-dependent properties of chemically doped graphene on PET under ambient conditions: (a) Optical transmittance (%T), (b) sheet resistance (R_S) of doped graphene, (c) Ratio of optical conductivity to dc electrical conductivity, and (d) the comparison of the ratio to other conductive transparent media. [15].

To assess the time evolution of the doping, the $\%T_{550}$ and R_S were measured immediately after doping and at fixed time points thereafter, as illustrated in Figure 3(a) and (b). An ideal transparent conductor necessitates time invariant $\%T_{550}$ and R_S. However, as previously reported [8b, 9b], although dopants reduce the sheet resistance, they also often reduce the optical transmittance. For all samples, the transmittance decreased following doping, as shown in Figure 3(a). After exposure to air for 200 hours, undoped graphene maintained its initial transmittance and sheet resistance with only a small reduction (Δ%T = -0.8% and ΔR_S = -4.53 Ω/sq.). For the transmittance of the doped samples, a recovery process was observed, with the transmittance tending to increase, though only marginally so, with time. The most substantial increase was observed for $AuCl_3$-doped graphene (Δ%T = 1.9%). This increase is presumed to be associated with time-dependent desorption of physisorbed dopants, activated by ambient thermal excitation.[9c, 16] Desorption also underpins the variation in R_S, however it seems to a much lesser extent. The increase in R_S, for $AuCl_3$-doped graphene, was largely negligible (0.85 kΩ/sq. → 0.93 Ω/sq.). The largest time-dependent change in R_S was observed for $FeCl_3$-doped graphene (1.81 kΩ/sq. → 2.26 Ω/sq.). All doped samples showed an increase in R_S though often by comparatively small shifts.

The ratio of the optical conductance, σ_{opt}, to the DC electronic conductance, σ_{dc}, defines a figure of merit of the opto-electronic performance of transparent conductors, and can be estimated from; [15a, 17]

$$T = \left[1 + \left(\frac{tZ_0}{2}\right)\sigma_{opt}\right]^{-2} = \left[1 + 188.5\frac{1}{R_S}\left(\frac{\sigma_{opt}}{\sigma_{dc}}\right)\right]^{-2} \quad (5)$$

Here Z_0 is the impedance of free space (377 Ω) and t is the film thickness. For an ideal transparent conductive electrode $\sigma_{opt}/\sigma_{dc} \rightarrow 0$; this necessitates a low sheet resistance and concurrently high optical transmittance. The approximate σ_{opt}/σ_{dc} values of our doped transferred graphene, alongside competing transparent flexible conductors, are plotted in Figure 3(c) and (d), respectively. Low σ_{opt}/σ_{dc} means the material has low sheet resistance with high optical transmittance. For all doped samples $\sigma_{opt}/\sigma_{dc} < 1.40$. $\langle\sigma_{opt}/\sigma_{dc}\rangle = 0.74$ for the $AuCl_3$ during the entire measurement period. Though still someway off the industry standard (0.029), these unoptimised devices show promise. Our surface metrology suggests that dopant agglomeration at defects and grain edges are critical in healing the otherwise imperfect, non-contiguous transferred graphene, with $AuCl_3$ doping being the most efficient of the M_xCl_y considered.

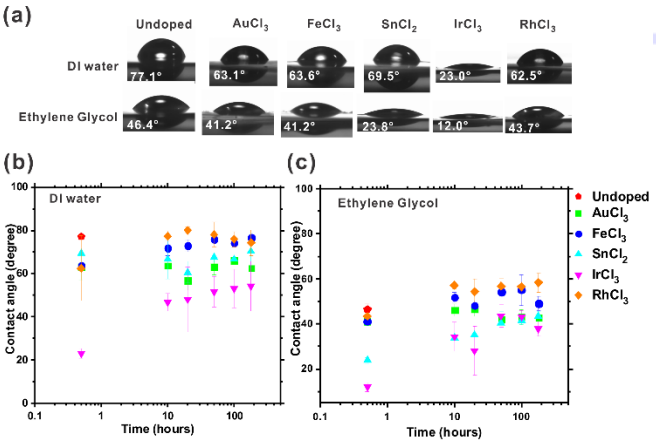

Figure 4. (a) Photographs of water and ethylene glycol droplets on chemically doped graphene for measuring contact angle. Time dependent contact angle using; (b) DI water, and (c) ethylene glycol.

During casting dopant molecules are physically adsorbed onto the graphene. Due to the inhomogeneous nature of molecular

binding, we believe that the surface energy of the graphene increases following chemical doping. The contact angle of undoped and doped graphene samples were measured using water and ethylene glycol probes (CAM200, LOT-Oriel Ltd.). The time-dependent contact angle with water is shown in Figure 4(b). Initially, after doping the contact angle decreased from 76.4˚ (undoped) to 63.1˚ ($AuCl_3$), 62.6˚ ($FeCl_3$), 69.5˚ ($SnCl_2$), 23.2˚ ($IrCl_3$), and 62.5˚ ($RhCl_3$). After exposure to air for 200 hours, the contact angle increased in $FeCl_3$ (76.7˚), $RhCl_3$ (74.3˚) and $IrCl_3$ (54.2˚), whereas there is no substantial change in the $AuCl_3$ (62.5˚) or $SnCl_2$ (70.3˚) cases. The surface energy can be calculated by substituting the Young's equation, $\gamma_S = \gamma_{LV}\cos\theta + \gamma_{SL}$ into the Owens-Wendt model[18] to give;

$$d\gamma = -\sum_i \Gamma_i d\mu_i \qquad (6)$$

Here γ_{SL} is the surface energy of the interface of the solid surface and liquid, γ_{LV} is the surface energy of the liquid, γ_S is the surface energy of the solid ($= \gamma_S^d + \gamma_S^p$), γ_S^d is the dispersion term of the surface energy of the solid, γ_S^p is the polar term of surface energy of the solid, γ_{LV}^d is the dispersion term of surface energy of the liquid, and γ_{LV}^p is the polar term of the liquids surface energy. At room temperature and ambient pressure, the surface energy of water is 72.8 mN/m ($= \gamma_{LV}^d + \gamma_{LV}^p$ = 24.7 + 48.1) and ethylene glycol is 48.3 mN/m ($= \gamma_{LV}^d + \gamma_{LV}^p$ = 30.9 + 17.4)[19].

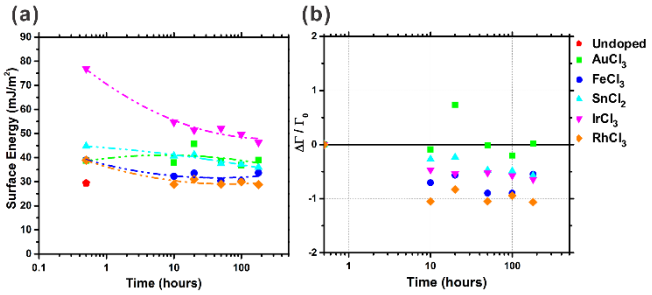

Figure 5. Time-dependent variation of (a) surface energy and (b) surface concentration of chemically-doped graphene with metal chlorides.

As plotted in Figure 5(a), the surface energy of undoped graphene is 29.4 mJ/m^2. After doping this increased to 38.8 mJ/m^2 ($AuCl_3$), 39.0 mJ/m^2 ($FeCl_3$), 44.7 mJ/m^2 ($SnCl_2$), 76.9 mJ/m^2 ($IrCl_3$) and 38.9 mJ/m^2 ($RhCl_3$). After 200 hours, the surface energy decreased for; $FeCl_3$ (33.7 mJ/m^2), $SnCl_3$ (36.0 mJ/m^2), $IrCl_3$ (46.3 mJ/m^2) and $RhCl_3$ (28.8mJ/m^2). This change in surface energy is consistent with our earlier %T and R_S. When graphene is metal chloride doped, there is a measurable increase in surface energy due to the deposition of local agglomerate precipitates, empirically verified by our surface energy measurements and corroborated by our measured decreases in %T and R_S. After 200 hours, some of the adsorbed molecular agglomerates of $FeCl_3$, $SnCl_2$, $IrCl_3$ and $RhCl_3$ are desorbed upon air exposure with samples subsequently exhibiting a decrease in surface energy and increase in R_S. Conversely, $AuCl_3$ showed a slight increase in surface energy, even after 200 hours' of STP air exposure ($\Delta\gamma$ = 0.18 mJ/m^2). This increase seems to arise from not only the much smaller amount of the dopant molecule desorption than other four doped samples, but also possible atmospheric oxygen adsorption. Attachment of oxygen tends to increase the surface energy. To evaluate the amount of desorbed molecules, the change in surface concentration was calculated from the Gibb's isotherm equation[20];

$$\gamma_{LV}(\cos\theta + 1) = 2\left(\gamma_S^d\gamma_{LV}^d\right)^{1/2} + 2\left(\gamma_S^p\gamma_{LV}^p\right)^{1/2} \qquad (7)$$

where, γ and $d\mu$ are the surface energy and the change in chemical potential, respectively. Γ is the concentration of adsorbed molecules on the surface, and is termed the surface excess. At constant temperature Γ is given by[20];

$$\Gamma = -\frac{1}{RT}\left(\frac{d\gamma}{dlnC}\right)_T \qquad (8)$$

Using equation (8) the temporal variation of the surface concentration, $\Delta\Gamma$ in the doped graphene was calculated, and is shown in Figure 5(b). Γ_0 is the surface concentration at t = 0 s, immediately upon its doping, and C is the concentration of dopant solution.

Figure 5(b) highlights the marked migration in dopant molecules away from, and attached to, the graphene surface. A negative $\Delta\Gamma/\Gamma_0$ with decreasing Γ indicates that the molecules are desorbed from the surface, whilst positive $\Delta\Gamma/\Gamma_0$ suggests the adsorption of molecules. The desorption case is trivial, with the net migration of local absorbates, deposited during the doping process, away from the surface. For $AuCl_3$-doped graphene, $\Delta\Gamma/\Gamma_0$ = 0.019 (after 200 hours). Positive $\Delta\Gamma/\Gamma_0$ implies that impurities, likely ambient oxygen, are being adsorbed onto the

graphene surface with absorption rates well within the time-frame of study. The absorption of ambient oxygen on nanocarbons is well established[21]. On the other hand, the negative values of $\Delta\Gamma/\Gamma_0$ for $FeCl_3$-doped graphene (-0.549), $SnCl_3$-doped graphene (-0.572), $IrCl_3$-doped graphene (-0.644) and $RhCl_3$-doped graphene (-1.064) shows that there was increased desorption. These results are consistent with the temporal variation of resistance. The resistance increase was the lowest in $AuCl_3$-doped graphene (0.08 kΩ/sq.). Therefore, it is apparent that the resistance increase can be attributed to the desorption of dopant molecules which provide charge carriers. Polymer passivation or hermetic capping layers can be utilised to help prevent degradation in ambient conditions.

Conclusions

Metal chloride-doped graphene is a promising transparent conductor for flexible electronics. $AuCl_3$–doped graphene exhibits a conductance ratio (σ_{opt}/σ_{dc}) of 0.70 with only 0.01 increase after 200 hours. The surface energy and the concentration change of adsorbed dopant molecules($\Delta\Gamma/\Gamma_0$) were analysed from the contact angle measurement with two kinds of probes. The lowest $\Delta\Gamma/\Gamma_0$ was in $FeCl_3$-doped graphene (-0.942) demonstrating the largest amount of desorption of dopant molecules which causes the largest resistance increase (0.45 kΩ/sq.). The molecule desorption is deeply related to the degradation of electrical resistance of chemically doped graphene with metal chlorides. The experimental results indicate that metal chloride doping of graphene can be a useful step for its adoption in flexible electronics.

Acknowledgements

MTC thanks the Oppenheimer Research Trust for generous financial support.

Keywords: graphene, transparent flexible conductors, chemical doping, metal chloride, stability, surface energy, desorption, and adsorption.

References

[1] aS. K. Lee, K. Rana, J. H. Ahn, *J Phys Chem Lett* **2013**, *4*, 831-841; bX. Huang, T. Leng, M. Zhu, X. Zhang, J. Chen, K. Chang, M. Aqeeli, A. K. Geim, K. S. Novoselov, Z. Hu, *Sci Rep* **2015**, *5*, 18298.

[2] aT. M. G. Paradee, A. Christou, *IEEE Tran. Dev. Mater. Rel.* **2015**, *15*, 423; bQ. Zhang, Y. Di, C. M. Huard, L. J. Guo, J. Wei, J. Guo, *J. Mater. Chem. C* **2015**, *3*, 1528-1536.

[3] aK. S. Novoselov, A. K. Geim, S. V. Morozov, D. Jiang, Y. Zhang, S. V. Dubonos, I. V. Grigorieva, A. A. Firsov, *Science* **2004**, *306*, 666-669; bS. Bae, H. Kim, Y. Lee, X. F. Xu, J.-S. Park, Y. Zheng, J. Balakrishnan, T. Lei, H. Ri Kim, Y. I. Song, Y.-J. Kim, K. S. Kim, B. Ozyilmaz, J.-H. Ahn, B. H. Hong, S. Iijima, *Nat. Nanotechnol* **2010**, *5*, 574-578; cA. K. Geim, *Science* **2009**, *324*, 1530-1534; dX. Li, Y. Zhu, W. Cai, M. Borysiak, B. Han, D. Chen, R. D. Piner, L. Colombo, R. S. Ruoff, *Nano Lett.* **2009**, *9*, 4359-4363.

[4] aT.-H. Han, Y. Lee, M.-R. Choi, S.-H. Woo, S.-H. Bae, *Nature photonics* **2012**, *6*, 105-110; bS.-Y. Kim, J.-J. Kim, *Organic Electronics* **2012**, *13*, 1081-1085; cJ. Wu, M. Agrawal, H. A. Becerril, Z. Bao, Z. Liu, *ACS Nano* **2010**, *4*, 43-48.

[5] aJ. Lee, M. T. Cole, J. C. S. Lai, A. Nathan, *J. Dis. Technol* **2014**, *10*, 362-366; bK. Jaeho, I. Masatou, K. Yoshinori, T. Kazuo, H. Masataka, I. Sumio, *Appl. Phys. Lett.* **2011**, *98*, 091502.

[6] aP. Lin, W. C. H. Choy, D. Zhang, F. Xie, J. Xin, C. W. Leung, *Appl. Phys. Lett.* **2013**, *102*, 113303; bH. Park, P. R. Brown, V. Bulovic, J. Kong, *Nano Lett.* **2012**, *12*, 133-140; cY. Un Jung, S.-I. Na, H.-K. Kim, S. Jun Kang, *J. Vac. Sci. Technol. A* **2012**, *30*, 050604.

[7] S. Ray, *Applications of Graphene and Graphene-Oxide based Nanomaterials*, Elsevier Science, **2015**.

[8] aU. Dettlaff-Weglikowska, V. Skakalova, R. Graupner, S. H. Jhang, B. H. Kim, H. J.

Lee, L. Ley, Y. W. Park, S. Berber, D. Tomanek, S. Roth, *J. Am. Chem. Soc.* **2005**, *127*, 5125-5131; bF. Gunes, H. J. Shin, C. Biswas, G. H. Han, E. S. Kim, S. J. Chae, J. Y. Choi, Y. H. Lee, *ACS Nano* **2010**, *4*, 4595-4600; cA. Kasry, M. A. Kuroda, G. J. Martyna, G. S. Tulevski, A. A. Bol, *ACS Nano* **2010**, *4*, 3839-3844; dH. J. Shin, W. M. Choi, D. Choi, G. H. Han, S. M. Yoon, H. K. Park, S. W. Kim, Y. W. Jin, S. Y. Lee, J. M. Kim, J. Y. Choi, Y. H. Lee, *J. Am. Chem. Soc.* **2010**, *132*, 15603-15609; eX. Li, D. Xie, H. Park, M. Zhu, T. H. Zeng, K. Wang, J. Wei, D. Wu, J. Kong, H. Zhu, *Nanoscale* **2013**, *5*, 1945-1948; fH.-Z. Geng, K. K. Kim, C. Song, N. T. Xuyen, S. M. Kim, K. A. Park, D. S. Lee, K. H. An, Y. S. Lee, Y. Chang, Y. J. Lee, J. Y. Choi, A. Benayad, Y. H. Lee, *J. Mater. Chem.* **2008**, *18*, 1261-1266; gD. Hee Shin, J. Min Kim, C. Wook Jang, J. Hwan Kim, S. Kim, S.-H. Choi, *J. Appl. Phys.* **2013**, *113*, 064305.

[9] aM. S. A. Abdou, S. Holdcroft, *Chemistry of Materials* **1996**, *8*, 26-31; bR. Ishikawa, M. Bando, Y. Morimoto, A. Sandhu, *Nanoscale research letters* **2011**, *6*, 111; cK. C. Kwon, B. J. Kim, J.-L. Lee, S. Y. Kim, *Journal of Materials Chemistry C* **2013**, *1*, 2463-2469.

[10] M. H. Kang, W. I. Milne, M. T. Cole, *IET Circcuits, Devices & Systems* **2015**, *9*, 39-45.

[11] aK. K. Kim, S. M. Kim, Y. H. Lee, *Acc Chem Res* **2016**, *49*, 390-399; b*Compendium of chemical terminology*, 2nd ed., IUPAC, **1997**.

[12] S. Li, Y. Wang, C. Lai, J. Qiu, M. Ling, W. Martens, H. Zhao, S. Zhang, *Journal of Materials Chemistry A* **2014**, *2*, 10211-10217.

[13] J. A. Dean, *Lange's handbook of chemistry*, 15th ed., McGraw-Hill Book Company, **1979**.

[14] H. Chang, M. Saito, T. Nagai, Y. Liang, Y. Kawazoe, Z. Wang, H. Wu, K. Kimoto, Y. Ikuhara, *Scientific Reports* **2014**, *4*.

[15] aS. De, T. M. Higgins, P. E. Lyons, E. M. Doherty, P. N. Nirmalraj, W. J. Blau, J. J. Boland, J. N. Coleman, *ACS Nano* **2009**, *3*, 1767-1774; bA. E. Rakhshani, Y. Makdisi, H. A. Ramazaniyan, *J. Appl. Phys.* **1998**, *83*, 1049-1057.

[16] aS. Tongay, K. Berke, M. Lemaitre, Z. Nasrollahi, D. B. Tanner, A. F. Hebard, B. R. Appleton, *Nanotech.* **2011**, *22*, 425701; bH. Liu, Y. Liu, D. Zhu, *Journal of Materials Chemistry* **2011**, *21*, 3335-3345; cK. C. Kwon, B. J. Kim, J.-L. Lee, S. Y. Kim, *Journal of Materials Chemistry* **2013**, *1*, 253-259.

[17] S. De, P. J. King, M. Lotya, A. O'Neill, E. M. Doherty, Y. Hernandez, G. S. Duesberg, J. N. Coleman, *Small* **2010**, *6*, 458-464.

[18] D. K. Owens, R. C. Wendt, *Journal of Applied Polymer Science* **1969**, *13*, 1741-&.

[19] I. Moutinho, M. Figueiredo, P. Ferreira, *Tappi Journal* **2007**, *6*, 26-32.

[20] D. K. Chattoraj, *Adsorption and thee Gibbs surface excess*, Plenum Publishing Corporation, New York **1984**.

[21] aC. Mathieu, B. Lalmi, T. O. Mentes, E. Pallecchi, A. Locatelli, S. Latil, R. Belkhou, A. Ouerghi, *Phys. Rev. B* **2012**, *86*; bF. Nasehnia, M. Seifi, *Modern Physics Letters B* **2014**, *28*.

Table of Contents

ARTICLE

Time evolution of electrical resistance (a), surface concentration (b) of metal chlorides-doped graphene, and a scheme describing adsorption and desorption of dopant molecules.

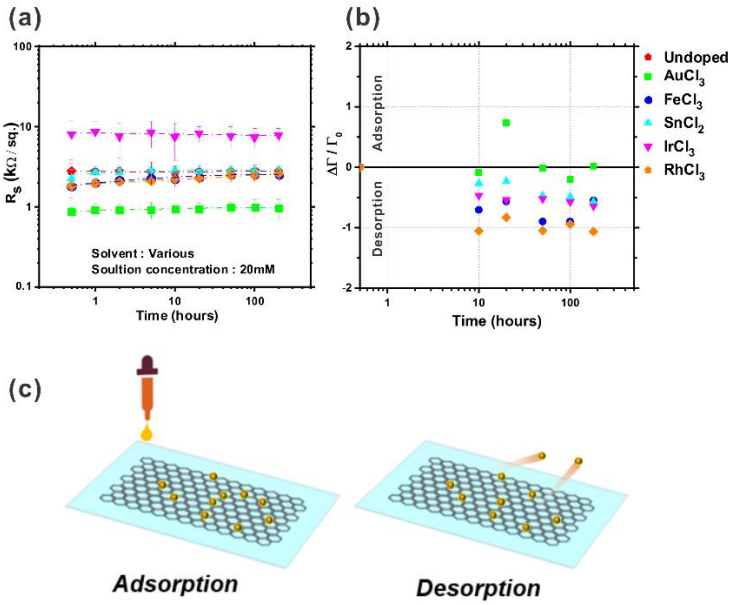

Moon H. Kang, William I. Milne, & Matthew T. Cole**

*Corresponding Author(s)**

Temporal Stability of Metal Chloride-Doped CVD Graphene